Sizing of Superconducting Cables for Turbo-Electric Distributed Propulsion Aircraft using a Particle Swarm Optimization Approach

S. Nolan, C. E. Jones, P. J. Norman, G. M. Burt

Abstract—Superconducting electrical power systems are proposed to meet high specific power densities required for turbo-electric distributed propulsion aircraft. Superconducting materials have unique thermal and electrical requirements for maintaining the superconducting state, which is critical to their normal operation. Electrical system faults can lead to this state being lost for all network assets in the electrical fault path. The resulting temperature rise can prevent the superconducting state from being immediately resumed following fault clearance, requiring disconnection of non-faulted equipment. Undersized cables experience a higher temperature rise under faulted conditions and disconnect from the system more readily. Oversized cables are heavier and more costly. Therefore, there is a need to optimize the cable size, preventing disconnection of equipment due to temperature rise following a fault whilst minimizing the weight and cost penalty.

This paper proposes a system parameter-driven methodology, utilizing particle swarm optimization, to identify fault tolerant cable designs, which deliver minimum through-life costs. This facilitates high-value, quantifiable design trade studies incorporating system parameters. Key observations drawn are that the choice between improving fault ride-through capability of a superconducting cable by increasing either the amount of superconducting material, or conventional former material, strongly depends on acceptable system operating temperature and voltage.

***Index Terms*—Superconducting, TeDP, electrical protection systems, aircraft electrical power systems,**

This paper was first submitted to IEEE Transactions on Transportation Electrification on 26th November 2021, and was accepted on 23rd April 2022. This work was supported by the Rolls-Royce University Technology Centre for Advanced Electrical Power Systems at the University of Strathclyde.

S. Nolan, C.E. Jones, P. J. Norman, and G. Burt are with the Department of Electronic and Electrical Engineering, University of Strathclyde, Glasgow, G1 1XQ, UK.
(e-mail:stevennolan646@gmail.com, catherine.e.jones@strath.ac.uk, patrick.norman@strath.ac.uk, graeme.burt@strath.ac.uk.).

I. Introduction

SUPERCONDUCTORS are a key enabling technology for future turbo-electric distributed propulsion (TeDP) concept aircraft. As opposed to traditional aircraft that use gas turbine engines to generate thrust, in a TeDP aircraft, thrust is provided by fans which are driven by electric motors. The required electrical power for the electrical motors is provided by generators driven by gas turbines. This approach allows for significant design freedom with respect to the placement and number of electrical motors and generators. Hence significant gains in overall aircraft efficiency can be made by utilizing this design freedom to take advantage of aerodynamically advantageous effects such as boundary layer ingestion (BLI) and increases in effective bypass ratio [1]. Through this, TeDP offers a route to meeting ambitious target reductions in greenhouse gases and noise of aircraft, as set out by NASA [2] and the EU [3]. However, a major challenge is to ensure that the larger electrical power system (EPS) required for these aircraft does not mitigate the general aircraft performance benefits of TeDP. For example, a 300 pax TeDP aircraft is expected to require in excess of 50 MW of electric power to take-off [4]. Superconductors have been proposed as a solution to reduce the overall mass of the electrical system [4]. As such, this paper focuses on a TeDP system utilizing Yttrium-Barium-Copper-Oxide (YBCO) based superconducting cables.

It is critical to resilient EPS design, that an appropriate protection system is implemented. This is underpinned by understanding the protection requirements for a particular system. There are five protection requirements defined in [5]: speed, sensitivity, selectivity, reliability and stability. To date, protection requirements for future superconducting systems are not well defined in the literature. However, it is not unreasonable to assume that superconducting cables will need to be able to provide the same level of fault ride-through capability as conventional components and ensure that electrical faults do not lead to significant isolation of the electrical network upstream of the fault location. For superconducting systems, these requirements are made more difficult by the need to

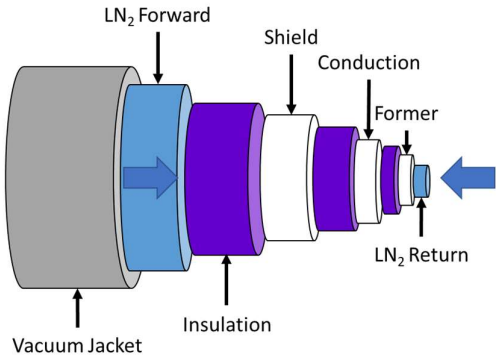

Figure 1. Illustration of superconducting cable's physical description.

maintain the superconducting state, which requires that the superconducting component is operated within strict thermal, electrical, and magnetic conditions that make up a boundary known as the critical surface [6]. Electrical faults can cause excursions above this boundary through exceeding the critical current, which can affect all components in the fault path, leading to energy being dissipated in the form of heat. This raises the temperature of superconducting distribution cables [7].

The interdependent nature of the critical parameters results in any increase in superconducting cable temperature leading to a temporary reduced maximum current that the cable is able to carry while maintaining the superconducting state [6]. Hence, if a component rides through the initial fault, it may still require removal from service due to it being unable to support the required load current without generating excessive heat as the increased temperature has reduced its maximum loading capacity [8]. In order for superconducting cables to provide safety margins that allow for fault ride-through capability, they must be sized appropriately with respect to four key variables: the size of the superconducting layer which affects the maximum value of the critical current; the size of the conventional cable former that provides an alternate path for current to flow through, the power rating of the cooling system to remove heat from the cable, and the speed at which the protection system can operate to interrupt the fault current.

Under-sizing superconducting components could lead to a damaging temperature rise during faults alongside limiting the power delivered to key network loads following a fault ride-through [8]. Conversely, over-sizing superconducting components causes an increase in weight and volume as well as capital cost. This is significantly detrimental to a superconducting distribution network for TeDP as it reduces the overall efficiency of the system: greater fuel burn per flight and greater number of flights required to recoup capital expenditure. This presents a multi-objective optimization problem between minimizing cable costs while maximizing system fault tolerance which this paper seeks to address.

This optimization approach determines the design of the superconducting and conventional materials for a fault tolerant cable design. An alternative to fault current tolerant design is to use the superconducting transition to create fault current limiting cables with high impedance that absorb fault energy [9]. However, this method requires long cable runs. The shorter lengths of cables on aircraft would lead to excess temperature rise during a fault, [10]. To date much of the research on cable stability has focused on cables using low temperature superconductors (<30 K operating temperature) for particle physics experimentation [11]. The authors of [11] provide a thorough overview of the techniques applicable for designing cables and measuring thermal stability of the material. However, in these conditions even small amounts of energy dissipation can lead to large temperature gains, and hence fault tolerance is difficult to achieve. High temperature superconductors that operate at temperatures close to or above that of the liquid nitrogen boiling point (77 K) have far greater thermal stability which allows for the design of fault current tolerant superconducting cables [9]. However, there is a significant gap in the research in the presentation of methods to optimize the sizing of cables for fault current tolerance with respect to key protection variables such as operating speed and system fault level. The paper is structured as follows: Section II provides the literature review for this paper; Section III describes the implementation methodology where the cable sizing problem scope is defined; Section IV presents the results obtained from the application of the optimization process which are then discussed in Section V; Section VI concludes this paper.

II. Optimization of Superconducting Components for Protection Requirements

A. Trade-off between super-conducing and conventional materials in superconducting cable.

The electrical power protection system influences the weight of a TeDP network directly through the mass of breakers, relays, fuses, and associated measurement and control equipment. The contribution that protection components have towards the total electrical power system weight for proposed TeDP architectures such as NASA's N-3X is considerable, as highlighted in [12], which demonstrates that up to 20% of overall system mass is due to protection equipment. However, protection requirements also indirectly increase the mass of the network through fault ride-through requirements in the form of fault level and interruption time (protection speed) impacting fault energy dissipation within non-faulted components, with the

former being dependent on the architecture and system variables, and the latter on the capabilities of the protection system to detect and remove the fault.

The speed at which the protection system can operate determines the length of time that superconducting components have to ride through faults. In future TeDP networks this will depend on the type of architecture adopted and technological advances in circuit breakers and metrology that may allow for faster detection and interruption of electrical faults. For instance, solid state protection systems have the potential to detect and remove faults from the system in time-scales of less than 1 ms [13]. However, there are constraints that must be overcome in the design of these devices before they can be used for the suggested electrical power levels of TeDP aircraft (50 MW) [4] include reducing device losses, and achieving required voltage ratings, surge current capability and power density [14]. Modern circuit breakers that are available for this power level aim to operate within a timescale of ten to hundreds of milliseconds [15]. If these are to be utilized in a TeDP architecture, the superconducting components must be designed to provide fault ride-through by ensuring that the fault-related temperature rise does not affect the ability to conduct full-load current after the fault is cleared, due to temperature rise suppressing the critical current of the superconducting component.

The fault ride-through capability of a superconducting cable is dependent on the size of the conventional (non-superconducting conductor, e.g. copper) and superconducting materials used in the construction of the cable, and the ability of the cooling system to remove excess heat [11]. Figure 1 shows an illustration of a typical superconducting cable which is comprised of a hollow conventional former, that acts as a conduit for a coolant path, separated from the superconducting tapes by a layer of insulation. Further insulation separates the conduction layer from a superconducting shield that prevents EMI, around which is a second coolant path. Having a larger amount of conventional material reduces the resistance of the shunt former while increasing heat capacity [11]. This reduces temperature rise during a fault at the expense of increasing capital cost and weight. Similarly, increasing the amount of superconducting material increases the critical current of the cable which is the maximum current the cable can carry before superconductivity is lost and ohmic heating occurs. Increasing the base critical current level of the cable allows for a greater temperature rise before critical current reduces below normal operating current. Hence, this approach increases fault ride-through capacity at the expense of greater capital cost due to the use of more superconducting material. However, due to the high current densities of superconducting materials, the impact on final component weight is negligible.

These factors create a trade-off, which requires optimization, between increasing the amount of superconducting material, leading to greater capital expense, and increasing the amount of conventional material, significantly increasing running costs, in order to achieve the appropriate fault ride-through capability for the application. Further, mass penalties in aviation are typically proportional to fuel price, which can vary significantly over time.

B. Optimisation and Sizing Methodology

To maximise the benefits of electrical propulsion, optimization of cable design is required to minimize the lifetime cost of the network in terms of initial capital expenditure and ongoing fuel costs due to network mass. However, given the thermal limits of superconducting components and the safety criticality of flight systems, the optimization method adopted must consider protection system operating speed and the impact of an electrical fault on the transient heating of un-faulted superconducting components in the fault path [8]. This is to prevent these components requiring isolation due to being unable to maintain the superconducting state once normal loading conditions resume.

One solution to this problem is presented in [8] which uses a control method that allows for cables that have exceeded the critical temperature for normal full load conditions to continue to operate in a reduced power mode. However, this is reliant on a back-up energy source or load shedding to be available to support network voltage stability [8]. This may not be possible in all architectures.

The impact of the cable shunt sizing on temperature rises during fault conditions is explored in [16] through the development of a 3-phase superconducting cable model that can be used for protection studies. However, the authors do not present a method for optimization of the shunt parameters with respect to protection requirements, weight, and cost.

To date, much of the optimization-based literature for superconducting components is focused on superconducting fault current limiters (SFCL) due to their technological maturity and applications in terrestrial networks. For instance, the authors of [17] consider the use of an analytical hierarchy process for the design of an SFCL to maximise limiting capability. Similarly, [18] explores the design of an optimal shunt impedance to improve transient response and system stability of a system containing SFCLs using a genetic algorithm.

However, a framework for optimizing superconducting cable parameters with respect to capital cost, weight, and system protection requirements within a DC mini grid for future aircraft electrical networks has thus far not been presented in the literature. Due to the wide variety of optimization variables and the complex

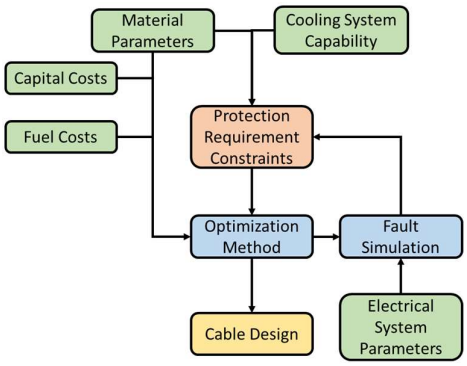

Figure 2. Methodology for minimisation of superconducting cable lifetime cost.

constraints that must be accounted for, a metaheuristic method such as particle swarm optimization (PSO) is a good candidate for finding solutions due to its low computational effort, simple implementation, ability to converge quickly and with a high probability of finding the global best solution [19]. This allows for more computational effort to be used in evaluating the constraints, which requires the simulation of a complex engineering system.

III. Description of Optimization Approach

A. Methodology

The superconducting cable sizing problem for TeDP requires that the cable configuration, in terms of superconducting and conventional material area, minimizes the lifetime cost of the cable. Costing must include consideration of both initial upfront and operating expenses. Operating expenses include impact on aircraft fuel consumption due to cable mass. The selected cable must also be able to withstand fault ride-through conditions and return to normal operation once a fault is cleared. Solving this cable sizing problem is dependent on several factors:

- Full load current requirement and operating voltage.
- Material constants: superconducting surface parameters, heat capacity, density, resistivity etc.
- Fault severity.
- Required protection system operating speed.
- Environmental conditions: operating temperature, cooling power.
- Cost of materials, manufacturing, and fuel.

These factors need to be accounted for in the optimization process to ensure that the cable is able to provide fault ride-through capability while ensuring cost-effectiveness. While each of the factors is important, later in the paper greater focus will be given to the impact of network operating voltage and protection system operating speed as these are key design variables within future aerospace architecture concepts [12]. Figure 2 shows the methodology proposed by this paper for the determination of optimal cable design.

As shown in Figure 2, environmental, electrical, protection, and material parameters are used within a fault simulation to determine whether the cable design found at any given point during the process breaks the constraints of the protection requirements, while the capital and operating costs (fuel burn due to cable weight) are used to evaluate the fitness of the solution selected. If at any time during the process, a selected cable design breaks the constraints, it is penalized through a penalty function.

The function for optimization used here is described by

$$f(S_{sh}, I_c) = K_{sh}S_{sh} + W_{sh}S_{sh} + K_{su}S_{su} + W_{su}S_{su} \quad (1),$$

where K_{sh} (£/m^2) is the capital cost coefficient of the conventional shunt materials and K_{su} *(£/m^2)* is the capital cost coefficient of the superconducting materials, defined in (2) and (3), S_{sh} *(m^2)*is the cross-sectional area of the conventional material, W_{sh} *(£/m^2)* [1.4] is the weight coefficient of the conventional material and W_{su} *(£/m^2)* is the superconducting weight coefficient, defined in (4) and (5), and I_c (A) is the critical current.

$$K_{sh} = \sigma_{cu} l_e M_{sh} \quad (2)$$

$$K_{su} = \sigma_{su} l_e M_{su} \quad (3),$$

$$W_{sh} = \sigma_{sh} l_e O \quad (4),$$

$$W_{su} = \sigma_{su} l_e O \quad (5),$$

where σ_{su} *(Kg/m^3)* is the density of the superconducting material, l_e *(m)* is the length of the cable, M_{su} (*£/kg*) is the capital cost per unit kg of the superconducting material and O (*£/kg*) is the cost of fuel per unit kg of material.

B. Fault Circuit Modelling

The electrical circuit used to model the rail-to-rail DC fault for each step of the algorithm is shown in Figure 3. While this model will not capture all the transient effects of the electrical fault, the two key contributors to temperature rise are accurately captured by the bandwidth of this model. These are the capacitive discharge of the power electronics filter and the following steady state fault current. It is assumed that electrical power is generated on the TeDP aircraft from a generator, driven by a gas turbine. This power is converted to DC by a rectifier, interfacing to a DC distribution system. The superconducting cable is modelled with superconducting material in parallel with a metallic

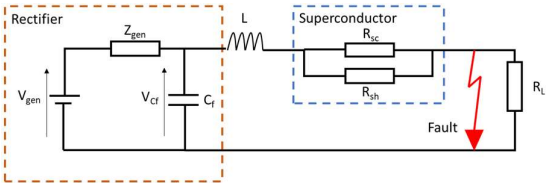

Figure 3. Circuit model used for fault simulations.

former. Upstream, a constant DC voltage source behind an impedance represents a generator-fed rectifier. In the event of a rail-to-rail fault, the DC link capacitor, C_f, will discharge, significantly influencing the peak fault current size and shape. Sustained, lower magnitude fault current is provided by the generator interfaced through the rectifier to the DC section of the system.

The impedance of the generator, Z_{gen} *(Ω),* is determined by the apparent power of the generator, S_{gen} *(VA)*, and the operating voltage, V_{gen} *(V),* is calculated by

$$Z_{gen} = \frac{V_{gen}^2}{S_{gen}} \quad (6).$$

It is assumed that the inductive component of the impedance of the generator is significantly greater than the resistive portion. Hence the resistive element of the impedance of the generator is neglected. The inductance, L_{gen}, is calculated by

$$L_{gen} = \frac{Z_{gen}}{2\pi f_{gen}} \quad (7),$$

where Z_{gen} is the impedance of the generation source, and f_{gen} is the frequency of the generated voltage. The size of the DC link filter capacitor, C_f *(F)*, is calculated for a voltage source converter using (8) ,

$$C_f = \frac{S_{gen}}{V_{gen}^2} \frac{6}{\frac{2\pi}{6} f_{sw}} 6 \quad (8),$$

where f_{sw} (*Hz*) is the switching frequency of the rectifier [20]. The differential equations for the circuit shown in Figure 3 are

$$V_{L_{gen}} = L_{gen} \frac{di_{gen}}{dt} \quad (9),$$

$$V_c = C_f \frac{di_c}{dt} \quad (10),$$

$$\frac{di_f}{dt} = \frac{V_c(t) - i_f(t)\left(R_{fault} + R_{cable}(t)\right)}{L_f} \quad (11),$$

where V_{Lgen} is the voltage across the generator impedance, L_{gen} the inductance of the generator, i_{gen} is the current through the generator impedance, V_c is the voltage across the DC filter capacitance, i_c, is the current going into the capacitor, and L_f is the size of the cable inductance. The initial condition of the circuit has the capacitor charged to network voltage and the current through the inductor at full load level when the fault is applied. These equations are solved for each time-step using MATLAB's ode45 solver to determine the fault current, i_f *(A),* through the superconducting cable by solving (11). The resistance of the superconducting portion of cable, R_{sc} *(Ω)*, is determined by (12) and updated at each timestep,

$$R_{sc}(t) = \frac{E_c \left(\frac{I_{sc}(t)}{I_c(T)}\right)^n}{I_{sc}(t)} l_e \ (12),$$

where E_c *(V/m)* is quench voltage constant, $I_{sc}(t)$ [1.14]is the instantaneous current in the superconducting material, I_c *(T)[1.14]* is the temperature-dependent critical current, n is the transition index, and l *(m)* is the length of the cable. The temperature dependent critical current is calculated from (13),

$$I_c(T) = I_{cref} \left(\frac{Tc - T}{Tc - Tr}\right)^k \quad (13),$$

where I_{cref} is the critical current at the reference temperature, T_{ref}, and k is the temperature dependence index of the critical current.

At each time-step, the total impedance of the superconducting cable is determined using an iterative current sharing algorithm that first calculates the amount of current in the superconducting layer and the conventional former [21]. Then the total resistance of the parallel combination is calculated. It is assumed that the cable has a uniform critical current and the superconducting and conventional material are treated as lumped element models as shown in Figure 3. Whilst for large cables with variations in critical current, the amount of heat dissipated could vary locally, which can lead to the temperature of the cable being non uniform across its length. However at this stage of the design process a uniform value for the critical current is sufficient as the use of a highly conductive stabilizer, such as copper, will ensure this variation in temperature is insignificant.[26]. The temperature of the cable, T_{cable} *[1.14](K)*, is then calculated as

$$T_{cable}(t) = \frac{1}{C_{pi}} \int_0^t Q_{in}(t) - Q_{out}(t)\, dt \quad (14),$$

where Q_{in} *(J)* is the ohmic losses produced by current in both the conventional and superconducting layers that are dissipated in the cable and Q_{out} *(J)* is the heat removed by the cooling system, calculated by (15)

$$Q_{out} = hA\Delta T \quad (15),$$

where h is the heat transfer coefficient, A is the area of the cable and ΔT is the temperature difference between the cable and the coolant. The heat capacity, C_{pi} *(K/J)*, and resistance of shunt built into the cable, R_{shunt} *(Ω)*, are determined by the size of the shunt cross-sectional area (CSA), A_{shunt} *(m^2)*, and the fundamental properties of the material in accordance with (15) and (16) respectively,

$$R_{shunt} = \frac{\rho l_e}{A_{shunt}} \quad (15),$$

$$C_{pi} = A_{shunt} l_e C_{vi} \quad (16),$$

where l *(m)* is the length of the cable, ρ *(Ω·m)*[1.17] is the resistivity of the material, C_{vi} *(J/m^3)* is the volumetric heat capacity. This continues until the stopping point of the simulation is reached. This is determined by the circuit breaker operating time. The temperature reached during the simulation is then passed back to the main optimization loop to

determine if the cable configuration meets the operating constraints.

C. Optimization Implementation

For this paper, the authors chose to use PSO to minimize the lifetime cost of the superconducting cables because it uses a simpler approach than other optimization methods. This allows more computational effort to be spent on constraints, which requires the simulation of a thermal-electric superconducting cable model under electrical fault conditions, although this process can be run offline while ensuring the search space of possible solutions is adequately explored [19]. PSO consists of a set number, or swarm, of particles moving through a search space in which every location is a potential solution to the objective function that requires optimization [19]. Each particle uses knowledge of its own best solution and that of the swarm as a whole in order to navigate this solution space before converging on the best answer found by the swarm. This allows for an efficient search process much quicker than brute force methods [19].

In order to find the global minimum or maximum within this search space each particle tracks the location of its personal best-known solution, P_{best}, and the best-known solution that any particle within the swarm has managed to find, G_{best}. Upon every iteration of this technique the objective function is evaluated for each particle, i, and their current position, X, in each dimension, j, is updated according to their current location and the answer to the velocity vector, v

$$v(i,j) = \delta v(i,j) + r_1 c_1\big(P_{Best} - X(i,j)\big) + r_2 c_2\big(G_{Best} - X(i,j)\big) \quad (17).$$

In (16) the correction coefficients c_1 and c_2 describe the cognitive and social capacity of the particles respectively, defining essentially how much the particle wants to move in the area of its personal best solution and how much the particle wants to move toward the best-known location within the swarm. It is this communication between individual particles and the overall swarm that allows for convergence to occur. R_1 and r_2 are random numbers between *0* and *1* that adds a random element into the movement of the particles. δ is the inertia of the particle, the amount the particle wants to move in the direction its currently pointed toward. Positions are updated on each iteration of the technique according to

$$X(i,j) = X(i,j) + V(i,j) \quad (18).$$

Figure 4 shows a flow diagram for the optimization process and describes that at each iteration of the optimization a fault simulation is carried out for each cable configuration stored in the particle's location data: the size of the superconducting layer; the size of the cable shunt area, as determined by (18). The particles fitness is then updated according to (1) before any penalties are applied using the constraints procedure described in section III D. Particle velocities are updated according to (17) and the process begins again until the particles converge on the best solution found by the swarm.

D. Constraints handling

To prevent the PSO process from producing unviable results, a constraint handling procedure is required. This first requires definition of the constraints themselves. These are defined as follows:

- At nominal operating temperature, the cable must be able to provide the maximum operating current without quench occurring. Before the fault: $I_c\ (T_{cable}) > I_o$ *for* $T_{cable} == T_{nom}$
- Following the fault, the cable must be able to supply a percentage, k, of the full load current without quench occurring. After the fault: $I_c\ (T_{cable}) > k\ I_o$ *for* $T_{cable} == T_{pf}$

The first constraint is that the critical current of the cable must be large enough so that the cable does not quench in normal operation. The second constraint ensures that the cable has fault ride-through capability so that in the event that a fault happens downstream on the network, it is able to provide

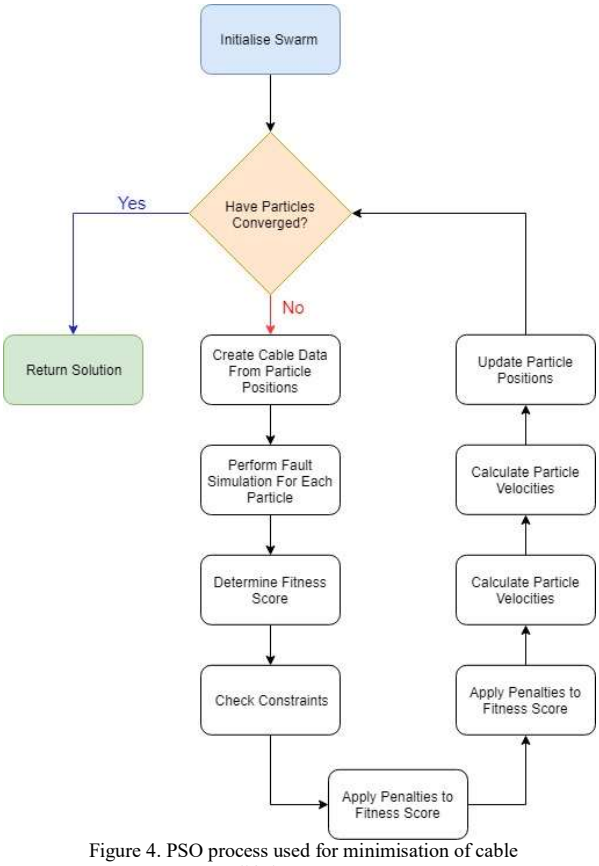

Figure 4. PSO process used for minimisation of cable lifetime cost.

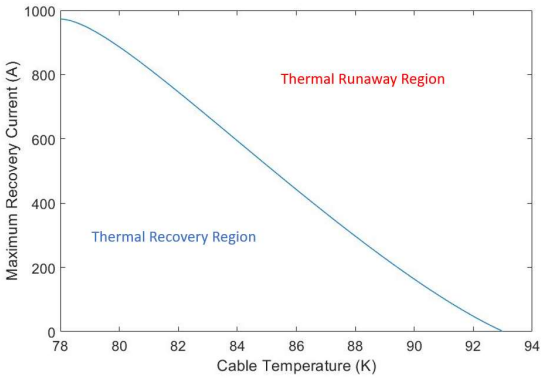

Figure 5. Example of relationship between MRC and cable temperature.

some portion of the full load current without thermal runaway. This will normally be the maximum operating current but could be reduced if the system has a significant number of redundant paths and energy storage to allow for reduced power flow on the affected feeder while the cooling system removes excess heat. This would have the benefit of reducing the volume, and weight, of each cable.

Determining whether the particle breaks the second constraint is achieved by determining the maximum temperature the cable reaches during the fault and checking if it is greater than the maximum recovery temperature (MRT) for the required load current. The MRT is the maximum temperature that the component can reach while still being able to carry a set amount of current, the maximum recovery current (MRC), without thermal runaway occurring [8]. As the temperature of a superconducting cable increases, the MRC decreases due to the inverse nature of the critical current to critical temperature and the limitations of the cooling system to remove excess heat. Figure 5 shows an example of the relationship between cable temperature and MRC for a superconducting cable with I_c of 1000 A at 77 K [8].

Due to the nature of the PSO process, some particles will be in the infeasible region, the area of the search space where solutions do not satisfy the constraints, of the solution space. This is the part of the search area in which solutions violate constraints. Due to the invalidity of these solutions, it is undesirable for convergence to take place within this area. To prevent this a number of strategies have been developed for PSO, from which, the authors in [22] provide an overview of many of the most commonly adopted ones. The implementation presented in this paper uses a dynamic penalty function. This punishes particles for entering the infeasible region. The penalty functions are given in (19) and (20), where Υ is the penalty given for each constraint, τ is the penalty multiplier, I_{cmin} (A) is the minimum critical current under normal conditions, I_{ci} (A) is the critical current in normal conditions for particle i, I_{MRCreq} (A) is the maximum recovery current required by the system, I_{MRC} (A) is the maximum recovery current of particle i after the fault simulation, n is the iteration number, and M is the maximum number of iterations.

$$\gamma_{i_1} = \tau_1\left(I_{c_{min}} - I_{c_i}\right)\frac{n}{M} \qquad (19)$$

$$\gamma_{i_2} = \tau_2\left(I_{MRC_{req}} - I_{MRC_i}\right)\frac{n}{M} \qquad (20).$$

The penalty reduces the fitness score of a particle and thus discourages particles from searching that area for a solution. The penalty function penalizes the particle relative to both the iteration number and the amount by which it exceeds the constraint. By implementing the penalty function this way the particles can more easily explore areas near the infeasible region early in the algorithm. This is beneficial as many of the best solutions can often be located on the boundary of the feasible region. As the iteration number increases, the function ensures that particles are discouraged from staying in the infeasible solution space.

TABLE I: BASE-CASE PARAMETERS FOR ALGORITHM IMPLEMENTATION

Parameter	Value	Symbol [1.7]	Parameter	Value	Symbol
Number of Particles	12		Power Level [8]	10 MVA	S_{gen}
Maximum Iterations	100		Fault Impedance [8]	10 mΩ	R_{fault}
Number of Swarms	3		Former Resistivity [25]	2 nΩ.m	R_{sh}
Fault Simulation Time Step	0.001 s		Cable Length [8]	100 m	l_e
Post Fault Current Requirement	100 %	k	AC Frequency[8]	50 Hz	f_{gen}
Superconducting Material [8]	YBCO		Former Cost Coefficient [23]	$4.05	M_{sh}
Coolant Temperature	65 K	T_{Cool}	Superconductor Cost Coefficient	$400.5	M_{su}
Heat Transfer Coefficient	0.2 W/mK	h	Weight Factor [24]	50	O
Critical Temperature [8]	93 K	T_c	Heat Capacity [25]	185 J/m^3	C_{pi}
Density [26]	8940 kg/m^2	σ_{sh}	100 m Cable Inductance	10 μH	L_f

IV. Results

The parameters for the study are shown in Table 1. Where data is available in the literature it has been used. The liquid nitrogen is assumed to be kept at 65K, as it is in a liquid state at this temperature. For each case selected, which present different voltage levels used for the superconducting distribution network, the PSO algorithm is run three times. This is to reduce the chance that a sub-optimal result is returned due to particles gravitating towards local minima in the search space. Through observation, it was found that the algorithm was able to find the best result in the search space no less than two out of three times. The output of a swarm is two cable parameters: conventional shunt material area and a superconducting critical current. From the base case described in Table 1, which considers a 10 MW subsection of a TeDP system, the voltage is varied between *1 kV* and *10 kV* in steps of *250 V*. The particles are allowed to select values for the shunt former in steps of *10* mm^2 while they can select the I_c in intervals of *100 A*. This ensures only discrete values are selected and helps prevent flat basin situations wherein multiple regions of the search space have very similar fitness, causing convergence speed to reduce. A timestep of *1 ms* is used. While a smaller timestep would provide greater accuracy of the fault transient, the vast majority of the heating takes place during the steady state fault period which this time step is sufficient to capture. The impact of a larger amount of insulation required at higher voltage has not been considered.

The cost of copper is assumed to be *$4.05/kg* [23], which was the market price for the metal at time of study. The cost of the YBCO tape is assumed to be approximately two orders of magnitude greater than the cost of the copper core. The weight factor, (4) & (5), multiplies the cost of materials based on mass, in an attempt to simulate the cost of fuel, which can vary widely depending on a large range social, economic, and political factors. This is set at *50* based on an estimate by an airframer that every *1 kg* of mass on an aircraft, the aircraft requires an extra *50 kg* of fuel over the course of a year [24].

Figure 6 shows the MRC of each cable selected, for a given voltage, at the post-fault operating temperature after a fault that is cleared in *1 ms*. The red line is the maximum full load current for the case in question at each voltage level. This is a strong indicator that the algorithm is successfully able to find global optimal solutions as there is no spare current carrying capacity: following the fault the cable is only able to support the full load current without thermal runaway taking place. Similarly, any decrease in the CSA or critical current will cause the MRC to drop below the red line, breaking the post fault current carrying requirement constraint, rendering the solution invalid. Other Pareto optimal solutions may exist within the solution space, however exploring the Pareto front for this problem is not the goal of this paper.

Figure 7 shows the overall cost of the cable solution selected by the optimization algorithm at different voltage levels and fault ride-through time requirements. Figures 8 and 9 show the critical current size and shunt CSA respectively, at each voltage level and protection requirement, while Figure 10 shows the peak temperature reached by

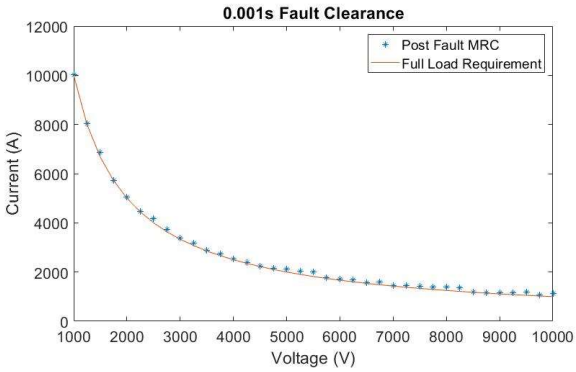

Figure 6. Comparison of post fault MRC of solution found by the optimization algorithm, and the full load requirement at that voltage level.

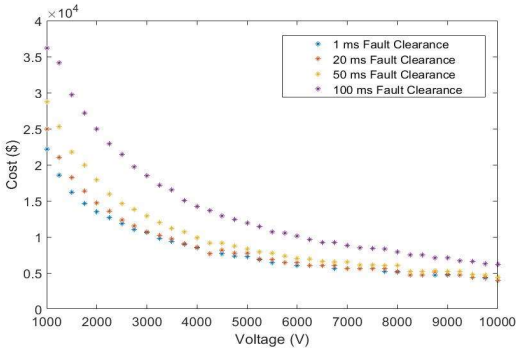

Figure 7. Overall cost of cable with respect to voltage and fault ride-through requirements.

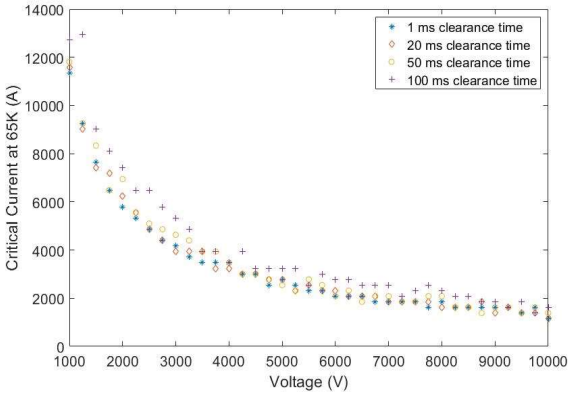

Figure 8. Critical current size selected by the optimization algorithm for different voltage and fault ride-through times.

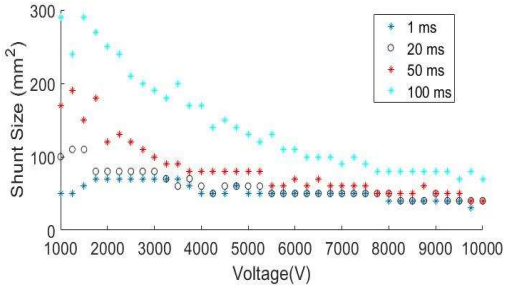

Figure 9. Shunt CSA selected by the optimization algorithm for different voltage and ride through times.

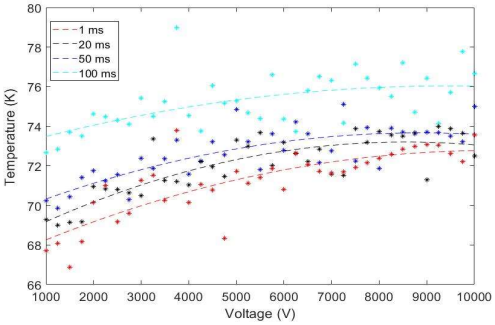

.

Figure 10. Peak temperature reached during selected cable configuration's fault simulation.

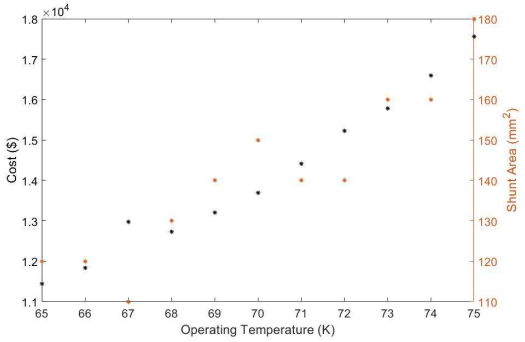

Figure 11. Variation in cost and CSA of conventional shunt with respect to operating temperature.

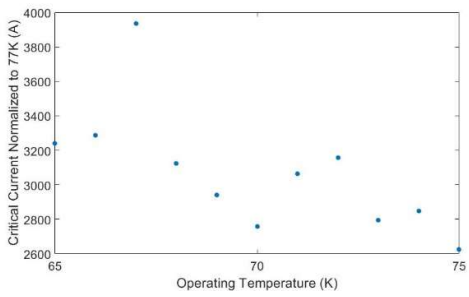

Figure 12. Relationship between critical current and operating temperature for optimized cable configuration [4.6].

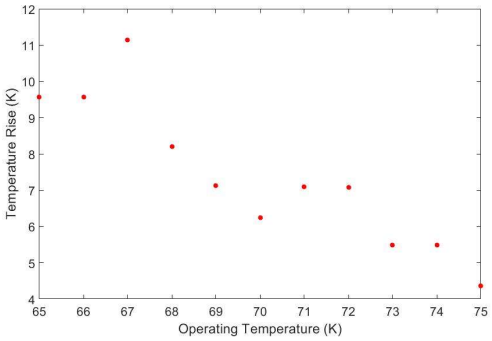

Figure 13. Temperature rise in cable by selected PSO solution for different operating temperatures.

the cable during the selected configuration's fault simulation. Figures 11 and 12 show how operating temperature affects the output of the optimization algorithm in terms of cost, CSA, and I_c selected as the cable choice.

V. Discussion

It can be seen in Figure 7 that increasing voltage can reduce the cost of the cables required, with the effect being more pronounced at lower voltages. This is due to steady state current carrying requirements reducing in line with increasing network voltage, reducing the critical current and CSA requirements of the cable and therefore cost. However, as the clearance time increases, the cost of the superconducting cable selected by the optimization method increases for each network voltage due to requiring a larger conventional and superconducting CSA to absorb the greater amount of energy that must be absorbed by the cables due to withstanding fault current for a longer period of time. This also demonstrates the impact that fast-acting protection equipment can have on reducing costs in future aircraft electrical systems by reducing cable size requirements.

Figure 8 indicates that critical current sizing decreases as the voltage increases, this is primarily due to reduced operating current for the same power level, while longer fault durations require greater base critical current. This ensures that the superconductor's MRC does not drop below the required load due to the higher temperatures reached by the component during these fault durations as shown in Figure 10. Greater temperatures occur as the optimization algorithm determines that a greater critical current base, according to the parameters of the case study in Table 1, is a less expensive solution than preventing greater temperature rise through an increase in shunt area. Similarly, as with the critical current, increases in voltage cause a decrease in the size of the conventional shunt required. From the best fit lines in Figure 10, it can be seen that peak

temperature generally increases with voltage level, and this is more pronounced at faster interruption times. An explanation for this effect is the greater impact of the capacitive discharge on temperature rise at higher voltages where there is more energy stored on the capacitor, and fast interruption times where there is less contribution from steady state fault current. As shown in Figure 10, longer interruption times shift the peak post-fault temperature of the cable selected up, with the optimization algorithm converging on solutions that use more superconducting material to offset this temperature rise depressing post fault critical current, Figure 8.

The influence of steady state operating temperature on the superconducting cable affects the results of the PSO algorithm in multiple ways as shown by Figures 11, 12 and 13. The underlying impact that operating temperature has on the circuit is the critical current density of the superconducting tape (higher at lower temperatures), and the size of the energy gap between the operating temperature and the critical temperature, where superconductivity is no longer possible (also larger at a lower operating temperature). As such, increasing the normal operating temperature of the superconducting cable leads to more superconducting material being required to maintain superconductivity at the same current level.

As shown by Figures 11, 12, and 13, temperature is varied from the base case of *65 K* to *75 K*. The fault ride through requirement is set at *100 ms* for all of these cases. Figure 11 shows the cost of the cable configurations found by the PSO algorithm and it can be seen that as the operating temperature increases, the cables' cost increases as well. This cost however does not consider any additional cooling costs required to keep the cables at lower temperatures. Shown on the right axis of Figure 11 is the shunt area size requirement which can be seen to be rising broadly in proportion to the cost of the cable configuration, indicating its more beneficial on a lifetime cost basis at higher temperatures for the cable to be able to absorb greater fault energy rather than increase the amount of superconducting tape.

In contrast, the amount of superconducting tape in the selected cable configuration decreases, in general, as the operating temperature increases and this is exemplified on Figure 12 which shows the critical current for each operating temperature, normalized to *77 K*. This indicates that as the temperature decreases it is more favorable to reduce the amount of conventional material, and therefore the weight of the component, and take advantage of the greater energy gap due to the larger difference between the operating and critical temperatures. The utilisation of this energy gap is exemplified in Figure 13 which shows the temperature rise following ride through for each operating temperature. As shown in this figure, a greater temperature rise is evident at lower operating temperatures, and this is primarily due to the lower heat capacity of the cable configuration selected. As well as the greater energy gap, the critical current density is greater at lower temperatures meaning that each additional Ampere of critical current is effectively cheaper. The impact of the additional cooling requirements would need to be considered to conduct a full cost analysis, but this is beyond the scope of this paper.

VI. Conclusion

TeDP presents an opportunity to reduce fuel burn through novel propulsion system architectures and the application of superconducting materials to electrical components. To maximise this, components must be optimized with respect to capital costs and operating costs incurred by the upfront price of new technologies and the expected implications for fuel burn of the component mass.

This paper has presented and applied an optimization methodology for superconducting cables to minimize lifetime cost which allows for a wide variety of system thermal and electrical parameters to be considered while ensuring protection requirements, specifically fault ride-through capacity and interruption speed, are adhered to. It is found that the algorithm is able to successfully identify optimal solutions within the search space and that system variables have a significant impact on the final result. Specifically, this approach allows the sizing of the cable critical current and shunt stabilizer area, to be carried out with respect to any voltage level and operating current. It is found that faster operating times can significantly reduce the cost of the cables at all voltage levels considered in the case study through reduction in the amount material required for absorbing fault energy. Hence fast acting solid state circuit breaker technology is a key enabler for reducing the cost of superconducting systems. Additionally, this approach determined that lower cable operating temperatures allow for large reductions in cable material usage, although this has to be balanced against greater cooling requirements, the cost of which is not captured in this paper and may be an optimization variable of interest in future work.

Future implementations of this method will also aim to apply it to more complex network architectures to consider systems that contain multiple protection system operating points, such as in zonal protection systems, as well as multiple generation sources that may allow for greater recovery margins and reduced operation modes in cables that have had to withstand temperature rise due to an electrical fault.

REFERENCES

[1] M. Kero, "Turboelectric Distributed Propulsion Test Bed Aircraft," Rolling Hills Research Coporation, El Segundo, *Tech. Rep.,* 2013.

[2] E. Greitzer, P. Bonneyfoy, E. De la Rosa Blanco, and E. Al, "Volume 1 : N + 3 Aircraft Concept Designs and Trade Studies," NASA, Tech. Rep. March, 2010.

[3] M. Darecki, C. Edelstenne, T. Enders, E. Fernandez, P. Hartman, J. Herteman, M. Kerkloh, I. King, P. Ky, M. Mathieu, G. Orsi, G. Schotman, C. Smith, and J. Worner, "Flightpath 2050, Europe's Vision for Aviation", 2011. [Online]. Available: http://ec.europa.eu/transport/modes/air/doc/flightpath2050.pdf

[4] H. D. Kim, G. V. Brown and J. L. Felder, "Distributed turboelectric propulsion for hybrid wing body aircraft", Proc. Int. Powered Lift Conf., pp. 1-11, 2008.

[5] ALSTOM, "Network Protection and Automation Guide", Alstom Grid, 2011.

[6] S. M. Blair, "The Analysis and Application of Resistive Superconducting Fault Current Limiters in Present and Future Power Systems," Ph.D. dissertation, University of Strathclyde, 2013.

[7] K. Sivasubramaniam, T. Zhang, A. Caiafa, X. Huang, M. Xu, L. Li, E. T. Laskaris, and J. W. Bray, "Transient capability of superconducting devices on electric power systems," *IEEE Transactions on Applied Superconductivity*, vol. 18, no. 3, pp. 1692–1697, 2008.

[8] S. Nolan, C.E. Jones, P. Norman et al. "Voltage-Based Current-Compensation Converter Control for Power Electronic Interfaced Distribution Networks in Future Aircraft", *IEEE Transactions on Transport Electrification*, vol. 6, no. 4, Dec 2020.

[9] C. E. Bruzek, A. Allais, K. Allweins, D. Dickson, N. Lallouet, and E. Marzahn, "Using superconducting DC cables to improve the efficiency of electricity transmission and distribution networks", *Superconductors in the Power Grid*, Elsevier Ltd, 2015.

[10] S. Nolan., P. Norman, C. Jones and G. Burt, "Protection Requirements Capture for Superconducting Cables in TeDP Aircraft Using a Thermal-Electrical Cable Model," SAE Technical Paper 2017-01-2028, 2017, https://doi.org/10.4271/2017-01-2028.

[11] L. Bottura, "Cable stability," Cern, Geneva, Switzerland, Tech. Rep., 2014. [Online]. Available: https://cds.cern.ch/record/1974064/files/arXiv:1412.5373.pdf

[12] M. J. Armstrong, M. J. Blackwelder, A. M. Bollman, C. A. H. Ross, A. Campbell, C. E. Jones, and P. J. Norman, "Architecture, Voltage, and Components for a Turboelectric Distributed Propulsion Electric Grid", 2015, no. July 2015. [Online]. Available: https://ntrs.nasa.gov/search.jsp?R=20150014237

[13] C. Gu, P.Wheeler, A. Castellazzi, A. J. Watson, F. Effah, "Semiconductor Devices in Solid-State/Hybrid Circuit Breakers: Current Status and Future Trends". Energies 2017, 10, 495. https://doi.org/10.3390/en10040495

[14] R. Rodrigues, Y. Du, A. Antoniazzi and P. Cairoli, "A Review of Solid-State Circuit Breakers", *IEEE Transactions on Power Electronics*, vol. 36, no. 1, pp. 364-377, Jan. 2021, doi: 10.1109/TPEL.2020.3003358.

[15] X. Pei, O. Cwikowski, D. S. Vilchis-Rodriguez, M. Barnes, A. C. Smith and R. Shuttleworth, "A review of technologies for MVDC circuit breakers", *IECON 2016 - 42nd Annual Conference of the IEEE Industrial Electronics Society*, Florence, Italy, 2016, pp. 3799-3805, doi: 10.1109/IECON.2016.7793492.

[16] B. C. Sung, D. K. Park, J. Park and T. K. Ko, "Study on a Series Resistive SFCL to Improve Power System Transient Stability: Modeling, Simulation, and Experimental Verification," in *IEEE Transactions on Industrial Electronics*, vol. 56, no. 7, pp. 2412-2419, July 2009, doi: 10.1109/TIE.2009.2018432.

[17] R. Sharifi and H. Heydari, "Optimal design of superconducting fault current limiters for electrical systems," 2010 Second International Conference on Engineering System Management and Applications, Sharjah, United Arab Emirates, 2010, pp. 1-6.

[18] S. Alaraifi and M Moursi, "Design Considerations of Superconducting Fault Current Limiters for Power System Stability Enhancement". *IET Generation Transmission & Distribution*, 2017.

[19] J.Kennedy, R. Eberhart "Particle swarm optimization". In: Proceedings of IEEE international conference on neural networks. Perth, Australia, pp 1942–1948, 1995

[20] R. Ottersten, "On Control of Back-to-Back Converters and Sensorless Induction Machine Drives Department of Electric Power Engineering," Ph.D. dissertation, Chalmers University of Technology, 2003.

[21] W. T. B. de Sousa, "Transient Simulations of Superconducting Fault Current Limitters," Ph.D. dissertation, Federal University of Rio de Janeiro, 2015.

[22] A. Rezaee Jordehi, "A review on constraint handling strategies in particle swarm optimization". 2015, Neural Computing and Applications. 26, 2015.

[23] Kitco, "Copper Spot Price", Kitco Metals, Accessed on: 14/04/2021 [online] Available: http://www.kitcometals.com/charts/copper_historical_large.html

[24] Airbus, "Getting to grips with fuel economy, Airbus, October 2004 [Online] Available: https://ansperformance.eu/library/airbus-fuel-economy.pdf

[25] N. J. Simon, E.S. Drexler, and R.P. Reed, "Properties of copper and copper alloys at cryogenic temperatures", Final Report, National Inst. of Standards and Technology (MSEL), Boulder, CO (United States). Materials Reliability Div, 1992.

[26] Royal Society of Chemistry, "Copper", RSC, London. [Online] Available: https://www.rsc.org/periodic-table/element/29/copper

Steven Nolan received the B.Eng. degree (Hons.) in electronic and electrical engineering from the University of Strathclyde, Glasgow, U.K., in 2015. He was a researcher within the Institute for Energy and Environment, University of Strathclyde, before moving into a role in industry as an engineering consultant. His research interests lie in the modeling and simulation, design, control, and protection of future aircraft power distribution systems.

Catherine E. Jones (Member, IEEE) received the M. Eng. Degree (Hons) in electronics and electrical engineering from the University of Glasgow, Glasgow, U.K. in 2003, and the Ph.D. Degree in electrical engineering from the University of Manchester, Manchester, U.K. in 2006. She is currently a Chancellor's Fellow (Lecturer) with the Institute for Energy and Environment, University of Strathclyde, Glasgow, U.K. Her research interests include power system architectures, protection and grounding for compact

electrical power systems.

Patrick J. Norman received the B.Eng. degree (Hons.) in electrical and mechanical engineering and the Ph.D. degree in electrical engineering from the University of Strathclyde, Glasgow, U.K., in 2002 and 2009, respectively. He is currently a Reader with the Institute for Energy and Environment, University of Strathclyde. His research interests lie in the modeling and simulation, design, control, protection of aircraft secondary power offtake and distribution systems, microgrid, and shipboard power systems.

Graeme Burt (M'95) received the B.Eng. degree and Ph.D. degree from the University of Strathclyde, Glasgow, U.K., in 1988 and 1992, respectively. He is currently a Distinguished Professor of electrical power systems at the University of Strathclyde where he directs the Institute for Energy and Environment, directs the Rolls-Royce University Technology Centre in Electrical Power Systems, and is lead academic for the Power Networks Demonstration Centre (PNDC). In addition, he serves on the board of DERlab e.V., the association of distributed energy laboratories. His research interests include the areas of decentralised energy; electrification of propulsion; DC and hybrid power distribution; experimental systems validation.